

The 2^1A_g state of *trans,trans*-1,3,5,7-octatetraene in free jet expansions

Hrvoje Petek,^{a)} Andrew J. Bell,^{b)} Young S. Choi,^{c)} and Keitaro Yoshihara

Institute for Molecular Science, Myoaaaji, Okazaki 444, Japan

Brett A. Tounge and Ronald L. Christensen

Department of Chemistry, Bowdoin College, Brunswick, Maine 04011

(Received 6 May 1992; accepted 20 November 1992)

The one-photon excitation spectrum is the same, with the exception of significant differences

spectrum, previously assigned to the $2^1A' \leftarrow 1^1A'$ transition of *cis,trans*-1,3,5,7-octatetraene. However, comparison of the one- and two-photon fluorescence excitation spectra shows clearly that the carrier of the spectrum has inversion symmetry, as expected for *trans,trans*-1,3,5,7-octatetraene. The one-photon spectrum is built on $h\nu$ and $2h\nu$ electronic origins, which are origins of progressions in a_g modes, while the two-photon spectrum is due to a single progression in a_g modes starting from the $2^1A_g \leftarrow 1^1A_g$ electronic origin. The appearance of out-of-plane vibrations, possibly including torsions of the polyene framework,

lifetimes vary between 170 and 450 ns due to the dependence of radiative and nonradiative

of 2^1A_g excess energy is tentatively ascribed to *trans-cis* isomerization. This work

of *all-trans* linear polyenes are sufficiently large to allow the study of 2^1A_g states under isolated, unperturbed conditions.

I. INTRODUCTION

The electronic spectroscopy of *trans,trans*-1,3,5,7-octatetraene, a prototypical linear polyene, has provided a great deal of information on the electronic structure and dynamics of simple conjugated molecules.^{1,2} Tetraenes are the longest polyenes for which reliable *ab initio* calculations of these systems provide the basis for understanding the excited states of longer

cesses such as vision and bacterial and plant photosynthesis.^{4,5} Long polyenes also are being investigated for their applications as materials with useful nonlinear optical and electronic properties.^{6,7} To provide experimental benchmarks for a theoretical understanding of polyene excited states, it is desirable to study the properties of *trans,trans*-1,3,5,7-octatetraene under isolated conditions. Measurements of the photophysical and photochemical properties of octatetraene under low temperature, isolated conditions also provide a point of reference for investigating the effects of environment and substitution on the photophysical dynamics of polyenes.

The optical spectroscopy of linear polyenes is governed by two low-lying electronic states—the ionic 1^1B_u (S_2) state and the covalent 2^1A_g (S_1) state (C_{2h} symmetry labels often are applied to linear polyenes even when the molecules are in the gas phase).^{12–15} The 2^1A_g state and Kohler were the first to demonstrate that the lowest

to the strongly allowed, $1^1B_u \leftarrow 1^1A_g$, lowest unoccupied

(LUMO \leftarrow HOMO) transition predicted by simple molecular orbital theories.⁸ Their work proved that in most linear polyenes, the lowest energy excited state is 2^1A_g , for which the transition moment is too weak to observe $2^1A_g \leftarrow 1^1A_g$ spectra by conventional absorption techniques.⁸ Theoretical calculations by Shulten, Ohmine, and Karplus^{9,10} showed that the mixing of singly and doubly excited A_g configurations results in a lowering of the 2^1A_g energy below that of the 1^1B_u state.

Even though the cross section for absorption to the 2^1A_g state is small, it can be populated efficiently from the 1^1B_u state by internal conversion on femtosecond time scales.¹¹ Subsequent chemistry occurs in the longer lived

The rates of internal conversion and isomerization are determined by couplings among the S_0 , S_1 , and S_2 states and surface crossings which occur at large torsional angles.^{13–15}

The interactions between the ground state and lowest excited singlet states have a number of manifestations in high resolution absorption and emission spectra. The broad

^{a)}Present address: Advanced Research Laboratory, Hitachi Ltd., Hatoyama, Saitama 350-03, Japan.

^{b)}Present address: Department of Chemistry, The University of Southampton, Highfield, Southampton SO9 5NH United Kingdom.

^{c)}Present address: Department of Chemistry, Yale University, New Haven, CT 06511, USA.

spectra of tetracenes¹⁶⁻¹⁹ most likely are due to conical intersections between the S_2 and S_1 states and are consistent with $S_2 \rightarrow S_1$ internal conversion on subpicosecond time

efficient oscillator strength to be observed in fluorescence excitation spectra due to strong Herzberg-Teller coupling^{20,21} between the 1^1B_u and 2^1A_g states, which is in-

Zerbetto and Zgierski have shown that a_g C=C stretching as well as b_g out-of-plane distortions enhance nonradiative decay in butadiene.¹³ Vibronic coupling between S_1 and S_0 is manifested by anomalously high CC stretching frequencies in the S_1 state and correspondingly low CC stretching

reduction in the activation energies for *cis-trans* isomerization about C=C bonds in the S_1 state.^{1,2,14,15} The displace-

factors in absorption and emission. Large Franck-Condon factors and the high vibrational frequencies make C=C stretches good accepting modes for internal conversion.^{12,13,26,27}

tetraenes exhibit rapid nonradiative decay processes with activation energies of <200 and ~ 2000 cm^{-1} , respectively.^{20,21,28} These decays may be due to *cis-trans* isomerization and/or $S_1 \rightarrow S_0$ internal conversion. Since many of the photobiological functions of polyenes involve excited state, *cis-trans* isomerization, it is essential to understand the details of this process in model systems under vibronically resolved, collision-free conditions.

Most of the information on the low-lying electronic states of linear polyenes has been obtained in mixed crys-

enes and how these properties are influenced by solvent environment.³⁰⁻³² Also, because of its large transition moment, it has been possible to measure the one-photon ab-

vanishingly small S_1 state fluorescence quantum yields under isolated conditions.^{1,2,33}

Two recent developments have provided new tools for studying polyenes in molecular beams. Kohler and co-workers applied the resonance enhanced multiphoton ionization (REMPI) technique to detect $S_1 \leftarrow S_0$ spectra of *cis*-hexatriene³³ and several *cis* isomers of alkyl substituted

trienes.³⁴ The observation of only minor *cis*-isomer impurities was attributed to extremely small oscillator strengths for the symmetry forbidden $2^1A_g \leftarrow 1^1A_g$ transitions of

octatetraene isomers using two-color, resonance enhanced, two-photon ionization (2C-RE2PI).³⁵ This spectrum was assigned to the *cis,trans* isomer because only *cis* trienes had

fluorescence techniques also were applied to the trienes where nonradiative decay at very low excess energies could be deduced from fluorescence lifetimes and relative fluorescence quantum yields.²⁸

We report here the one- and two-photon $S_1 \leftarrow S_0$ fluorescence excitation spectra and $S_1 \rightarrow S_0$ emission spectra of

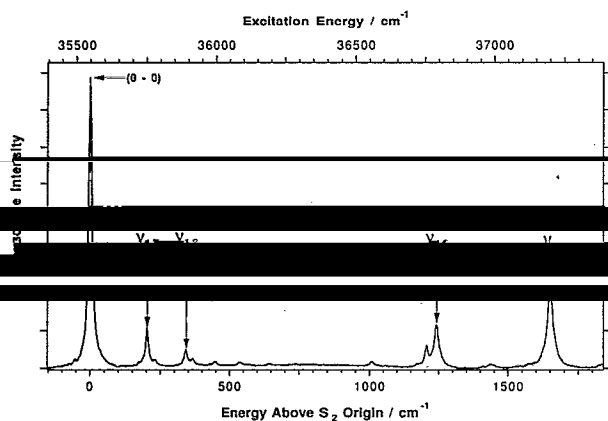
The one-photon $S_1 \leftarrow S_0$ spectrum is essentially the same as that observed in the 2C-RE2PI study,³⁵ but here is assigned to the *trans,trans*-octatetraene isomer. This is based

symmetry labels are strictly valid as expected for *trans,trans*-octatetraene. This assignment is further substantiated by careful examination of the one-photon, vibronically resolved $S_1 \rightarrow S_0$ spectra, including the analysis of

hot-band structure and comparison of vibrational frequencies with those observed in corresponding spectra of low temperature mixed crystals. These findings resolve the important question of whether the one- and two-photon cross sections of the $2^1A_g \leftarrow 1^1A_g$ transitions of *all-trans*-linear polyenes are sufficiently large to be detected under conditions where the center of molecular symmetry is rigorously maintained. Analyses of the $2^1A_g \leftarrow 1^1A_g$ spectra and the dependence of fluorescence lifetimes on vibronic energy level also provide new information on the structure and couplings between polyene electronic states and nonradiative decay processes (possibly including *trans* \rightarrow *cis* isomer-

II. EXPERIMENT

1,4,6-octatrien-3-ol at 80 °C using *p*-toluene sulfonate catalyst following the procedure of Yoshida *et al.*³⁷ yielded $>99\%$ isomerically pure *trans,trans*-1,3,5,7-octatetraene. Such high purity can be achieved because the dehydration procedure requires much lower temperature than in conventional synthesis.³⁶ Crystalline samples were kept at -80 °C before use in the experiments.



1,3,5,7-octatetraene in a He free jet expansion. The spectrum is presented to show the high isomeric purity of the *trans,trans*-octatetraene sample.

Since the $S_2 \leftarrow S_0$ absorption spectra of *trans,trans*-1,3,5,7-octatetraene are strongly allowed, the isomeric composition of the sample could be checked *in situ* by measuring the $S_2 \leftarrow S_0$ fluorescence excitation spectrum of our samples. Figure 1 shows the $S_2 \leftarrow S_0$ fluorescence excitation spectrum of the region where both isomers are expected to absorb. The spectrum is assigned exclusively to *trans,trans*-octatetraene based on the previous $S_2 \leftarrow S_0$ absorption,¹⁶ fluorescence excitation,¹⁷ and 2C-RE2PI spectra.³⁵ There is no feature corresponding to the *cis,trans*-1,3,5,7-octatetraene, whose $S_2 \leftarrow S_0$ origin was reported by Buma *et al.* at 73 cm^{-1} below the *trans,trans* origin.³⁵ Although the relative strengths of $S_2 \leftarrow S_0$ transitions and fluorescence quantum yields of the two isomers are not known, the observation of the $S_2 \leftarrow S_0$ fluorescence excitation spectrum of our sample suggests that the fluorescence technique has nearly the same

isomeric selectivity as the absorption technique.

From sample to sample, and decreasing with respect to the main isomer, the *cis,trans* isomer content was estimated to be

s,trans isomer. On the basis of the absence of *cis,trans*-1,3,5,7-octatetraene features in the $S_2 \leftarrow S_0$ fluorescence excitation spectrum, we conclude that our octatetraene sample contains <1% of the *cis,trans* isomer.

The experimental apparatus for measuring fluorescence excitation spectra, fluorescence spectra, and fluorescence lifetimes was essentially the same as previously used for experiments on methyl substituted trienes and tetraenes.^{19,28} The octatetraene concentration was controlled by fixing the sample reservoir temperature at 25°C for excitation spectra, $35\text{--}50^\circ\text{C}$ for emission spectra. Hof bands from population inversion of the S_2 state (350–480 Torr) were useful for estimating the energy of

the $S_1 \leftarrow S_0$ origin from one-photon excitation spectra. Stagnation pressures of $\sim 500\text{--}800$ Torr gave spectra of vibrationally and rotationally cold molecules. Under these experimental conditions, the octatetraene sample was sufficiently stable to make useful measurements for >12 h. Some polymerization may have occurred during the course of the experiments. However, the polymerization products did not interfere with the spectroscopic measurements.

Several overlapping scans from 347 to 300 nm using a Lambda-Physik EMG104/3002 excimer pumped dye laser with PTP and frequency-doubled outputs of sulforhodamine 101 and rhodamine B dyes. The excitation energy was <500 μJ and the laser beam collimated to ~ 2 mm diam to avoid saturation of transitions. A composite

of individual scans in the overlapping spectral regions. Laser scan intervals of 0.0025 nm between 347 and 314.5 nm and 0.005 nm between 314.5 and 300 nm gave sufficient reso-

lution. The $S_2 \leftarrow S_0$ spectrum was recorded using the second harmonic of the argon-ion 152 dye. Since the vibronic lines are much broader than for the $S_1 \leftarrow S_0$ transition, the laser scan interval was increased to 0.025 nm. The excitation energy had to be reduced to <1 μJ to prevent saturation of this strongly allowed transition. The optogalvanic spectrum of a Ne hollow-cathode lamp provided a wavelength calibration for the spectra. Excellent signal-to-noise ratios could be obtained by averaging ten laser shots at a 10 Hz repetition rate for each scan interval.

The two-photon $S_1 \leftarrow S_0$ spectrum was recorded from 691 to 674.5 nm using a Lambda-Physik LPX100/LPD3000 excimer pumped dye laser operating with pyri-

maline dye. The laser beam was focused by a 600 mm f1

lens with diameter 10 mm. A 250 mm focal

length lens with diameter 10 mm dispersed the emission, and an intensified multichannel diode array detector with a $25 \mu\text{m}$ spacing between elements (EG&G PAR 1420) recorded the spectrum with a resolution of $\sim 10 \text{ cm}^{-1}/\text{point}$. The input slit width was $100 \mu\text{m}$. Spectra were recorded by exciting the sample at a 15 Hz laser repetition rate and integrating the signal for 2–5 min. Emission from a low-pressure mercury lamp provided calibration spectra. Peak positions were determined by fitting Gaussian profiles to the observed lines.

The signal was recorded on a 9400 digital oscilloscope by summing 200–500 decay traces from a single photon excitation. The time resolution of the decay mea-

measurements was limited both by the 175 MHz bandwidth of the oscilloscope and the 15 ns pulse width of the excitation laser. Fitting the fluorescence decay profiles to single exponential decays gave the reported lifetimes. For higher energy vibronic states, it was necessary to convolute the laser pulse shape to extract accurate lifetimes. Since the

inversion symmetry in the *cis,trans* isomer. The $2^1A' \leftarrow 1^1A'$ transition of *cis,trans*-octatetraene is electric-dipole allowed for both one- and two-photon excitations. In both cases, optical transitions only couple bands of the same symmetry, and the one- and two-photon spectra should coincide. By contrast, the one-photon $S_1 \leftarrow S_0$ spec-

trons are estimated to be $<5\%$ for intense lines with $\nu > 1000 \text{ cm}^{-1}$ wavenumber based on comparison of

from vibronic coupling between the 1^1A_g and 2^1A_g states via b_u vibrations. Therefore, the one-photon $2^1A_g \leftarrow 1^1A_g$ spectra are restricted to transitions where the direct product of the initial and final vibronic states has b_u symmetry. Ab-

III. RESULTS AND DISCUSSION

One of the most important results of this study is to establish that the carrier of the spectra is *trans,trans*-

$S_1 \leftarrow S_0$ coupling induced by each mode. Franck-Condon promoting modes. Weaker bands may involve a_g transitions of several antisymmetric modes with an overall change corresponding to b_u symmetry. Emission spectra

tinguished from the *cis,trans*-octatetraene by the absence of

the $S_1 \leftarrow S_0$ electronic origin (Fig. 2) provides both the

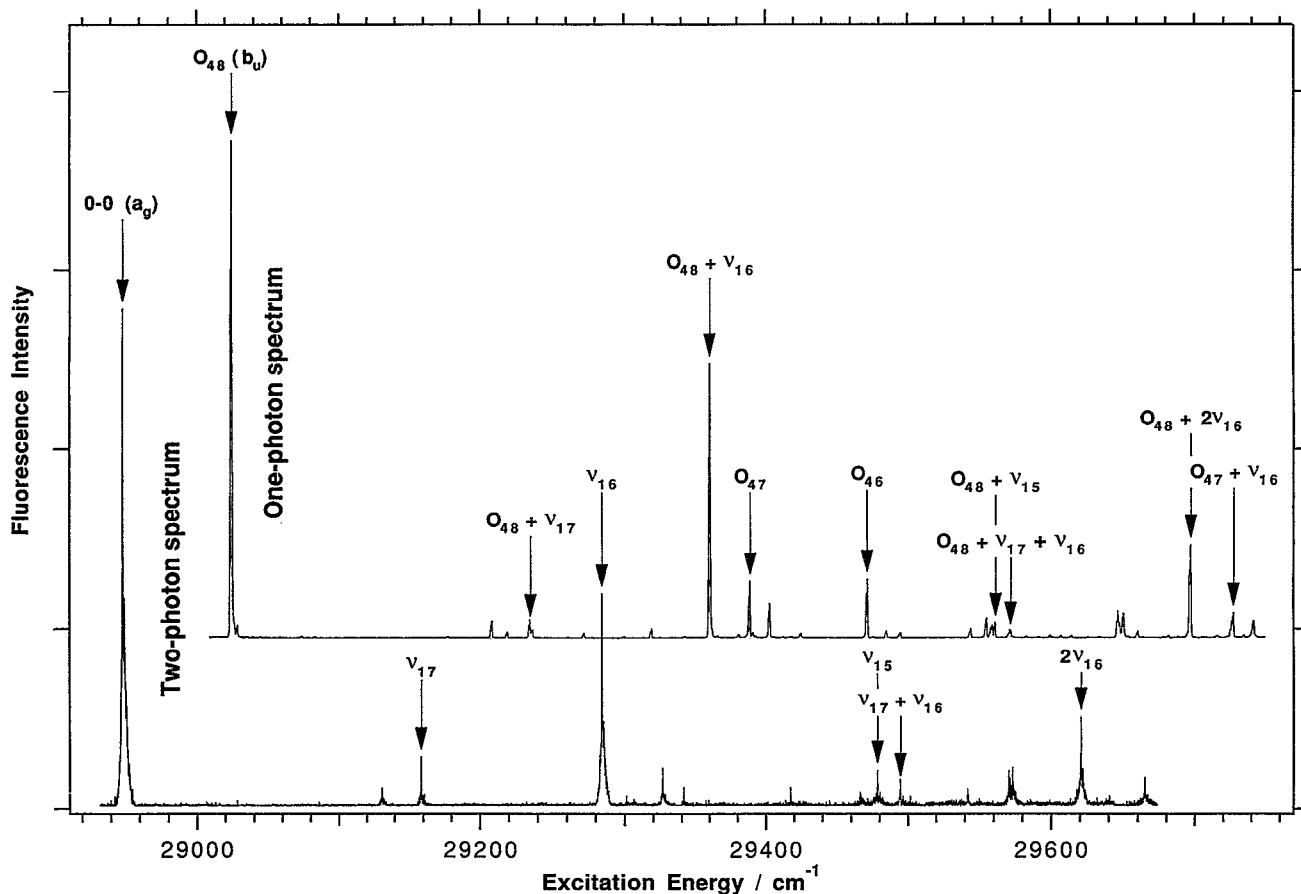


FIG. 2. A comparison of the one- and two-photon fluorescence excitation spectra of the $2^1A_g \leftarrow 1^1A_g$ transition of *trans,trans*-1,3,5,7-octatetraene. The assignments show that the two-photon spectrum is a progression in Franck-Condon active a_g vibrations and the one-photon spectrum is due to b_u .

TABLE 2. Observed, fundamental frequencies, combination bands, and overtones of the 2^1A_g state of *cis,trans*-octatetraene. The two-photon frequencies are measured relative to the 0-0 origin at $28\,948.7\text{ cm}^{-1}$ and the one-photon frequencies are measured relative to the 1-0 origin O_{48} at $29\,024.9\text{ cm}^{-1}$. For combination bands and overtones, Δ is the difference between the observed frequencies and the sum of the fundamental frequencies.

Two photon			b	
0-0	0			446
	182.4			442
ν_{17}	210.1			410
	212.4			
	247.0			
	294.5			
ν_{16}	336.0			434
	378.1			312
	469.1			
	518.4			221
ν_{15}	530.2			401
$\nu_{16} + \nu_{17}$	546.2	0.1		365
	593.7			262
	622.2			157
	623.2			163
	624.7			163
$2\nu_{16}$	672.4	0.4		395
	716.7			274
One photon				
ν_{48} ($1-0, b_u$)	(0)		(100.0)	341
<i>Cis,trans</i> ^c	33.4		0.2	
<i>Cis,trans</i>	48.8		0.3	281
$3\nu_{48}$	153.1		0.3	
	183.3		3.2	326
	193.9		1.2	377
$\nu_{48} + \nu_{17}$	209.7		3.5	337
	211.6		1.6	378
<i>Cis,trans</i>	235.9		0.1	
	246.8		0.8	315
	293.7		1.8	314
$\nu_{48} + \nu_{16}$	335.7		55.2	337
ν_{47} (b_u)	363.7		11.0	322
	377.8		6.6	297
$\nu_{48} + 2\nu_{17}$	419.2	-0.2	0.1	
ν_{46} (b_u)	446.7		11.6	318
	459.7		1.3	293
	469.9		0.9	305
	519.2		1.7	323
$\nu_{48} + \nu_{15}$	529.9		3.7	314
	532.7		1.8	373
	534.3		2.5	231
	536.2		2.9	203
$\nu_{48} + \nu_{16} + \nu_{17}$	546.0	0.6	0.8	
	547.5		1.2	352
$\nu_{47} + \nu_{17}$	574.6	1.2	0.7	
	621.9		5.1	170
	622.6		2.8	199
	625.2		4.7	219
	635.1		1.2	267
$\nu_{46} + \nu_{17}$	656.8	0.4	0.4	
$\nu_{48} + 2\nu_{16}$	672.2	0.8	18.5	331
$\nu_{47} + \nu_{16}$	700.8	1.4	3.1	277
	702.2		4.8	303
	716.7		3.3	289
	732.8		1.7	244
$\nu_{46} + \nu_{16}$	780.4	-2.0	9.8	322
	794.4		1.3	240
	805.0		4.3	316
	817.5		1.8	243
	824.4		1.5	303
$\nu_{48} + \nu_{15} + \nu_{16}$	865.8	0.2	2.5	284
	868.8		1.7	

TABLE I. (Continued.)

Assignment ^a	Frequency (cm ⁻¹)	Δ	Intensity	Lifetime (ns)
	870.5		8.7	231
	873.3	1.4	6.3	253
$\nu_{45} (b_u)$	875.4		5.1	240
$\nu_{10} + 2\nu_7 + \nu_9$	883.3	2.2	0.7	
	922.5		1.5	242
	957.8		2.2	227
$\nu_{48} + \nu_{14}$	964.8		4.3	242
$\nu_{44} (b_u)$	967.8		3.2	220
	970.2		5.2	258
$\nu_{46} + \nu_{15}$	978.6	2.0	1.0	
	1003.7		1.1	266
$\nu_{48} + 3\nu_{16}$	1009.1	2.0	3.2	286
	1061.0		1.1	248
$\nu_{48} + \nu_{13}$	1080.0		8.9	212
$\nu_{45} + \nu_{17}$	1084.4	-0.5	0.4	
$\nu_{45} + \nu_{16}$	1210.8	-0.3	4.2	196
$\nu_{48} + \nu_{12}$	1225.2		45.4	235
$\nu_{48} + \nu_{11}$	1275.5		8.4	203
$(\nu_{48} + \nu_{10})^d$	1279.6		4.9	201
$(\nu_{48} + \nu_9)$	1283.8		2.5	197
$\nu_{48} + \nu_{13} + \nu_{17}$	1289.1	0.6		
$\nu_{48} + \nu_{16} + \nu_{14}$	1300.0			
	1302.3		2.7	194
$\nu_{44} + \nu_{16}$	1303.5	0.0	2.2	
$\nu_{48} + 4\nu_{16}$	1343.3	0.5	0.1	
$\nu_{48} + \nu_{12} + \nu_{17}$	1436.5	1.6	1.0	
$\nu_{47} + \nu_{13}$	1444.2	0.5	1.6	
$\nu_{39} (b_u)$	1477.8		10.4	173
	1490.1		3.2	174
	1498.7		3.7	174
$\nu_{48} + \nu_7$	1508.7		8.8	169
$\nu_{38} (b_u)$	1515.0		18.7	171
$\nu_{46} + \nu_{13}$	1526.9	0.3	0.5	
	1532.3		3.3	169
$\nu_{45} + 2\nu_{16}$	1545.3	0.6	2.2	
$\nu_{48} + \nu_{12} + \nu_{16}$	1560.9	0.0	23.8	166
$\nu_{47} + \nu_{12}$	1588.3	-0.6	5.3	164
$\nu_{48} + \nu_{11} + \nu_{16}$	1610.8	-0.4	4.6	
$(\nu_{48} + \nu_{10} + \nu_{16})$	1615.4	0.1	2.1	
$(\nu_{48} + \nu_9 + \nu_{16})$	1619.4	-0.1	2.0	
$\nu_{47} + \nu_{11}$	1638.4	-0.8	2.5	
$\nu_{46} + \nu_{12}$	1670.9	-1.0	4.1	157
$\nu_{48} + \nu_{13} + 2\nu_{16}$	1752.0	0.6	1.4	
$\nu_{48} + \nu_{15} + \nu_{12}$	1755.3	0.2	1.6	
$\nu_{48} + 2\nu_{13} + 2\nu_{16}$	1758.9	0.4	1.8	
	1787.5		8.2	148
$\nu_{48} + \nu_6$	1797.9		92.0	145
$\nu_{38} + \nu_{16}$	1849.5	-1.1	15.1	137
$\nu_{47} + \nu_7$	1870.2	-1.4	2.6	140
$\nu_{48} + \nu_{12} + 2\nu_{16}$	1897.2	-2.2	7.0	137
$\nu_{47} + \nu_{12} + \nu_{16}$	1926.7	2.1	2.5	120
$\nu_{48} + 2\nu_{16} + \nu_{11}$	1947.3	0.4	1.1	
$\nu_{46} + \nu_7$	1954.2	1.2	1.5	
	1981.4	0.2	2.3	
$\nu_{48} + \nu_{17} + \nu_6$	2007.9	0.3	3.6	112
and/or $\nu_{46} + \nu_{12} + \nu_{16}$		0.3		110
and/or $\nu_{39} + \nu_{15}$		0.2		
	2029.6		2.4	109
$\nu_{48} + \nu_{14} + \nu_{13}$	2044.1	-0.7	0.8	
and/or $\nu_{38} + \nu_{15}$		-0.8		
	2046.4		1.0	100
$\nu_{48} + \nu_{16} + \nu_{15} + \nu_{12}$	2090.4		1.0	

TABLE I. (Continued)

Assignment ^a	Frequency (cm ⁻¹)	Δ	Intensity	Lifetime (ns)
$\nu_{45} + \nu_{12}$	2097.7	-2.9	1.1	58
	2123.0		2.1	59
$\nu_{48} + \nu_6 + \nu_{16}$	2132.7		17.1	60
$\nu_{39} + 2\nu_{16}$, and/or	2148.3	-0.9	1.9	49
$\nu_{45} + \nu_{11}$		-2.6		
$\nu_{48} + 2\nu_{13}$,	2158.2	-1.6	3.1	44
and/or $\nu_{47} + \nu_6$		-3.2		
	2174.9		1.6	44
$\nu_{38} + 2\nu_{16}$	2184.2	-2.2	0.9	44
$\nu_{44} + \nu_{12}$	2193.7	0.7	0.6	
	2216.3		1.1	78
	2221.0		0.9	58
$\nu_{48} + \nu_{12} + 3\nu_{16}$	2233.6	1.3	0.4	
$\nu_{46} + \nu_6$	2241.7	-2.9	1.7	28
$\nu_{48} + \nu_{12} + \nu_{13}$	2302.8	-2.4	0.5	21
$\nu_{15} + \nu_6$	2327.8	0.0	0.3	
	2337.2		0.7	19
	2430.3		1.3	13
$\nu_{48} + 2\nu_{12}$	2448.9	-1.5	2.2	12
$\nu_{48} + \nu_6 + 2\nu_{16}$	2467.2	-2.1	1.7	12
$\nu_{47} + \nu_6 + \nu_{16}$, and/or	2494.3	-3.0	0.6	
$\nu_{48} + 2\nu_{13} + \nu_{16}$		-1.4		
$\nu_{48} + \nu_{11} + \nu_{12}$	2498.3	-2.4	0.5	
($\nu_{48} + \nu_{12} + \nu_{10}$)	2503.3	-1.5	0.3	
$\nu_{46} + \nu_6 + \nu_{16}$	2573.8	-6.5	0.5	
	2668.4		0.8	7
$\nu_{48} + \nu_{12} + \nu_{13} + \nu_{16}$	2668.4	-4.9	0.8	7
$\nu_{45} + \nu_6$	2701.3	-1.7	0.5	7
$\nu_{39} + \nu_{12}$	2701.3	-1.7	0.5	7
	2784.8		0.7	
$\nu_{48} + 2\nu_{12} + \nu_{16}$	2784.8	-1.3	0.7	
$\nu_{48} + 3\nu_{16} + \nu_6$	2803.3	-1.7	0.2	
$\nu_{48} + \nu_{16} + \nu_{12} + \nu_{11}$	2834.6	-1.8	0.4	
$\nu_{48} + \nu_{13} + \nu_6$	2875.0	-2.9	0.5	
$\nu_{45} + \nu_6 + \nu_{16}$	3002.6	-4.3	0.5	
$\nu_{48} + \nu_{12} + \nu_6$	3020.3	-2.8	1.9	
$\nu_{39} + \nu_{12} + \nu_{16}$	3036.0	-2.7	0.2	
$\nu_{38} + \nu_{12} + \nu_{16}$	3073.5	-0.4	0.8	
$\nu_{48} + \nu_{16} + \nu_{13} + \nu_6$	3208.9	-4.7		
$\nu_{38} + \nu_6$	3267.3	-8.4	0.7	
$\nu_{38} + \nu_6$	3303.3	-9.6	1.0	
$\nu_{48} + \nu_{12} + \nu_6 + \nu_{16}$	3353.8	-5.0	0.7	
$\nu_{48} + 2\nu_6$	3577.6	-18.2	1.1	
$\nu_{48} + 2\nu_6$	3586.1	-9.7	0.9	
$\nu_{39} + \nu_6 + \nu_{16}$	3599.4	-12.0	0.3	
$\nu_{38} + \nu_6 + \nu_{16}$	3635.6	-13.0	0.4	
$\nu_{48} + \nu_{12} + \nu_6 + 2\nu_{16}$	3688.0	-6.5	0.1	
$\nu_{48} + 2\nu_6 + \nu_{16}$	3910.4	-21.1	0.6	
$\nu_{48} + 2\nu_6 + \nu_{16}$	3919.9	-11.6	0.3	
$\nu_{48} + 2\nu_6 + 2\nu_{16}$,	4243.4	-23.8	0.2	
and/or $\nu_{47} + \nu_6 + 2\nu_{16}$		-4.9		

^aThe vibrational numbering of Ref. 37 is used throughout the text.

^bTwo-photon spectra were not normalized for laser power, hence the relative intensities are not given.

^c"*Cis,trans*" indicates the bands which are thought to be due to the *cis,trans*-octatetraene impurity.

^dAssignments in parentheses should be considered as tentative.

simplest and the most compelling justification for the assignment of the carrier to *trans,trans*-octatetraene. The or-

lower in energy than the origin of the one-photon spectrum, the difference corresponding to one quantum of the lowest energy b_u mode ν_{48} (" O_{48} "). Identical shifts are

seen for many other bands. These correspond to a_g modes which appear in combination with ν_{48} in the one-photon

spectrum. Bands which do not have a counterpart in the two-photon spectrum are higher frequency b_u promoting modes such as ν_{47} and ν_{46} and their combination bands with a_g modes. The complete

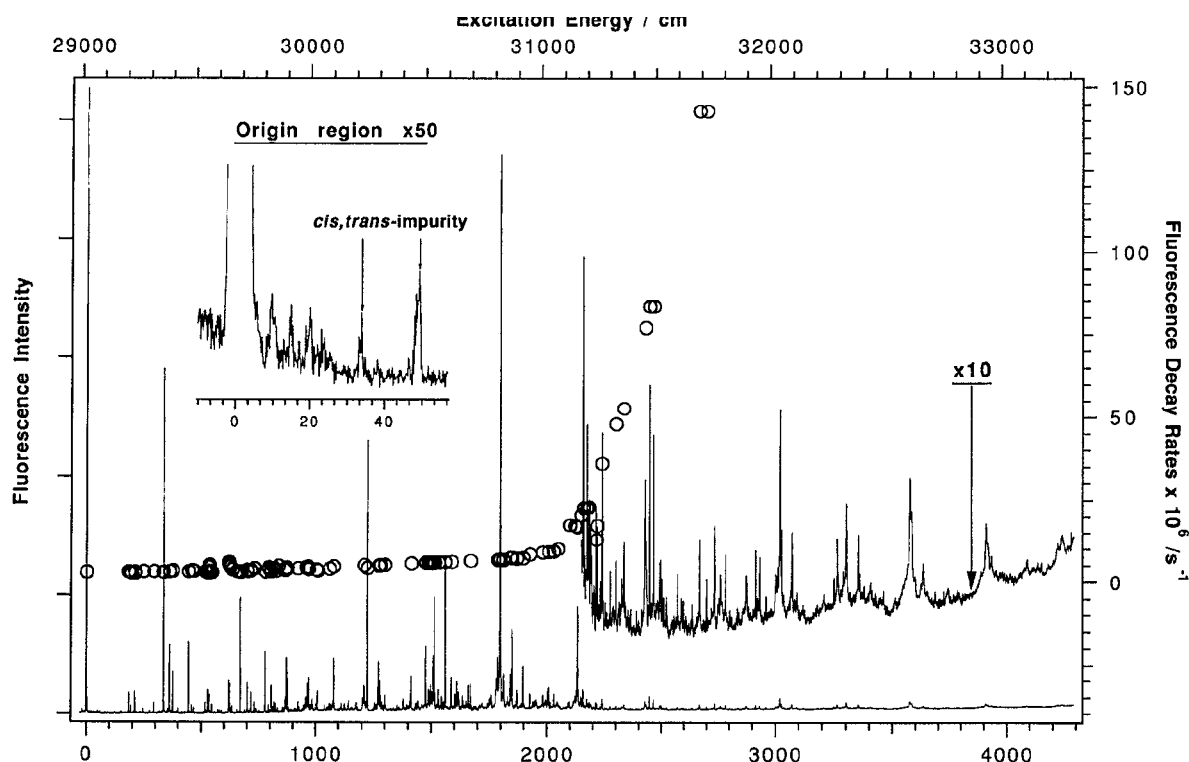


FIG. 3. The one-photon fluorescence excitation spectrum of the $2^1A_g \leftarrow 1^1A_g$ transition of *all-trans*-1,3,5,7-octatetraene in a He free jet expansion. The fluorescence decay rates of the stronger vibronic bands, which have been measured for some of the stronger transitions.

lack of overlap between vibronic bands in the two spectra proves that the one-photon ($g \rightarrow u$) and two-photon ($g \rightarrow g$) selection rules are strictly obeyed, excluding *cis,trans*-octatetraene as the carrier of the spectrum. The *cis,cis* iso-

isomer is significantly less stable than the other two isomers and none of the spectroscopic information suggests that it could be present. The energies, relative intensities, and lifetimes of the one- and two-photon spectra are presented in Table I. A more detailed analysis of the two-photon spectra of *trans,trans*-octatetraene will be presented in the future.

Further support for assigning *trans,trans*-octatetraene as the carrier comes from a variety of more conventional spectroscopic evidence: (i) comparison of $S_1 \leftarrow S_0$ absorp-

tion spectra with the $S_1 \leftarrow S_0$ spectrum of *trans,trans*-octatetraene will be crucial issue for studies of other polyenes for which the two-photon $S_1 \leftarrow S_0$ spectrum may be difficult to obtain.

B. Analysis of the one-photon $2^1A_g \leftarrow 1^1A_g$ spectrum

Figure 3 gives the one-photon fluorescence excitation spectrum of the $2^1A_g \leftarrow 1^1A_g$ transition of *trans,trans*-1,3,5,7-octatetraene in a He free jet expansion along with fluorescence decay rates of the stronger vibronic bands. A higher resolution spectrum covering the region 0–1000 cm^{-1} above the origin at 29 024.9 cm^{-1} is presented in Fig. 4, along with the fluorescence lifetimes. The assignment of the one-photon spectra in Figs. 3 and 4 to the symmetry forbidden $2^1A_g \leftarrow 1^1A_g$ transition of *trans,trans*-

trans,trans-octatetraene is supported by the following evidence:

(i) S_1 fluorescence lifetime measurements. Given the

known fluorescence lifetime of *trans,trans*-octatetraene

the inversion symmetry of octatetraene is rigorously main-

even without reference to the two-photon spectrum. This

tained).²⁴ room temperature infrared and Raman spectra

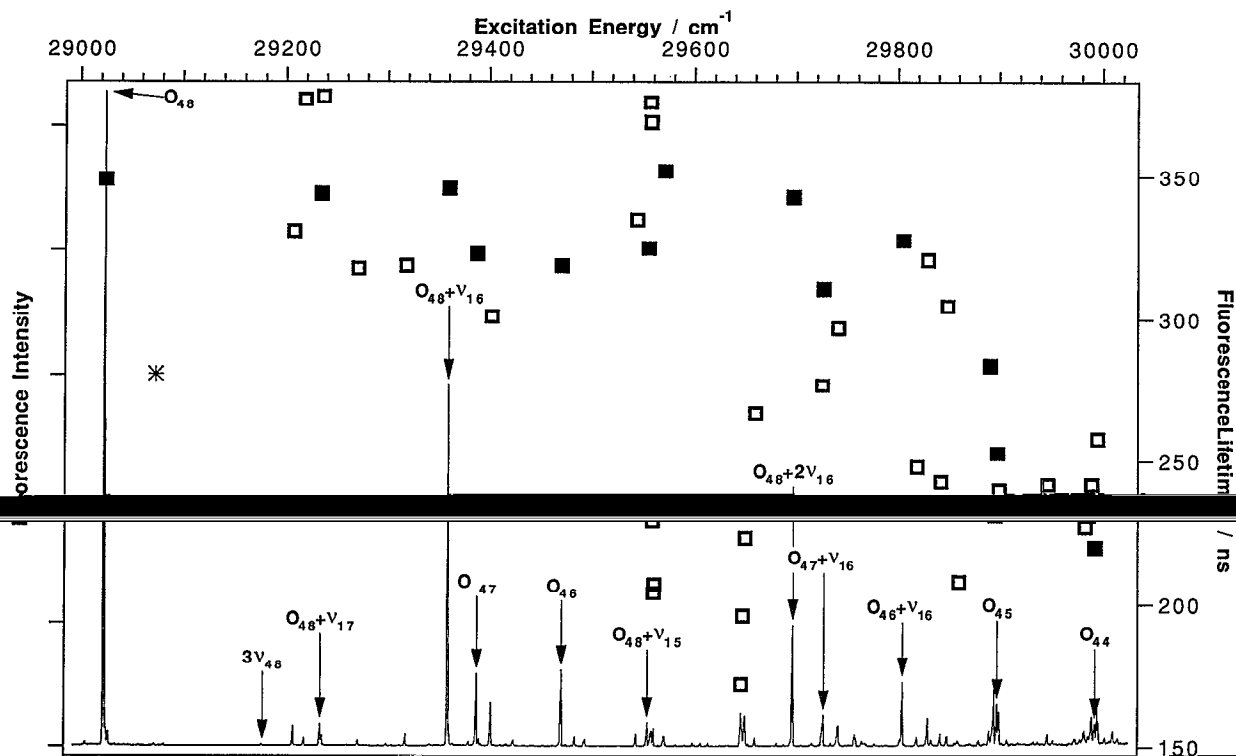


FIG. 4. An expanded portion of the spectrum in Fig. 3 showing the vibrational assignments and fluorescence lifetimes in the 0–1000 cm^{-1} spectral region above O_{48} , the $1 \leftarrow 0$ origin due to the excitation of one quantum in the b_u symmetry ν_{48} mode. Other b_u $1 \leftarrow 0$ origins are indicated in the same manner. Full squares represent the lifetimes for the assigned lines, open squares are for the unassigned ones, and the asterisk is for the *cis,trans*-octatetraene impurity. The lifetimes of assigned lines decrease with energy from 341 ns at the origin in a relatively monotonic manner, while the lifetimes of unassigned lines have considerably larger deviations from the average.

of the S_0 state,³⁷ and theoretical calculations.^{26,27} The S_1 and S_0 vibrational frequencies determined in this work are presented in Tables II and III together with previous condensed phase and theoretical frequencies which are the basis for assignments.

1. Assignment of the electronic origin of the

In this section, we use the hot-band structure of the one-photon spectrum to find the electronic origin of the $2^1A_g \leftarrow 1^1A_g$ transition and to show that the origin of the one-photon spectrum in Figs. 2, 4 is a $1 \leftarrow 0$ transition in the lowest energy in-plane bending ν_{48} vibration. The one-

photon vibronically allowed $2^1A_g \leftarrow 1^1A_g$ transition, the electronic origin of 2^1A_g only can be accessed by $\Delta v = -1$ excitation from b_u vibronic states of 1^1A_g . Since ν_{48}'' also is the lowest energy b_u promoting mode spectra of

in $\nu_{48}'': \Delta v = +1$ transitions will form a sequence starting with O_{48} , while $\Delta v = -1$ transitions will form another sequence starting from $0' \leftarrow 1''$ at an energy corresponding to $\nu_{48}'' + \nu_{48}'$ below the O_{48} . Condensed phase frequencies for

corresponding to three different vibrational temperatures.

from O_{48} and the $\Delta v = -1$ bands starting from 28 862.0 cm^{-1} . The discrepancy between the predicted and observed origins of the $\Delta v = -1$ sequence can be rationalized by the solvent dependence of ν_{48} frequencies in the ground

The relative intensities and the extent of vibrational

for assigning the sequence bands as shown in Fig. 5. The $\sim 10 \text{ cm}^{-1}$ shift to lower energy of successive members of each progression is due to a $\sim 10 \text{ cm}^{-1}$ decrease of the ν_{48} frequency in the S_1 state from its S_0 value. The shadings of rotational line shapes to high energy for $\Delta v = -1$ transi-

TABLE II. A comparison of frequencies of fundamental vibrations in the S_1 state determined for *trans,trans*-octatetraene and *cis,trans*-octatetraene in free jet expansions and mixed crystals. The *cis,trans*-octatetraene vibrational frequencies measured in mixed crystals are given next to *trans,trans* frequencies with the closest resemblance. All frequencies are in units of cm^{-1} .

Assignment	<i>Trans,trans</i> supersonic jet ^a	<i>Trans,trans</i> ^c supersonic jet ^a	<i>Trans,trans</i> ^d mixed crystal	<i>Cis, trans</i> ^e mixed crystal	<i>All-trans</i> theory ^f
a_g					
ν_{16}	335.7	336	341	393	334
ν_{15}	529.9	538	530	497	604
ν_{14}	964.8				958
ν_{13}	1080.0	1080			1137
ν_{12}	1225.2	1226	1221	1128, 1226	1220
ν_{11}	1275.5	1275	1271	1320	1267
ν_{10}	(1279.6) ^b				1323
ν_9	(1283.8)				1350
ν_8					1464
ν_7	1508.7	1509		1508	1487
ν_6	1797.9	1799	1754	1722	1711
ν_5					2982
ν_4					3063
ν_3					3077
ν_2					3083
ν_1					3095
b_u					
ν_{48}	76.2	76.2	93		106
ν_{47}	439.9	440	463		435
ν_{46}	522.9	524	538		590
ν_{45}	951.6				940
ν_{44}	1044.0	1044	1054		1054
ν_{43}					1195
ν_{42}					1240
ν_{41}					1320
ν_{40}					1357
ν_{39}	1554.0	1555			1463
ν_{38}	1591.2	1592			1543
ν_{37}					2981
ν_{36}					3063
ν_{35}					3079
ν_{34}					3089
ν_{33}					3099

^aThe frequency for ν_{48} of 76.2 cm^{-1} from this work has been used to calculate frequencies of all other b_u symmetry S_1 fundamentals measured in the

^bAssignments in parentheses should be considered as tentative.

^cReference 35.

^dReference 24.

^eReference 29.

^fReference 27.

by in-plane bending in the lower and upper states of the a sequence was deduced by observing the effect of vibra-

cues populating the low frequency bending and torsional modes. Although there are a number of S_1 vibronic states

with $< 500 \text{ cm}^{-1}$ energy, only ν_{48} appears with significant intensity because it is both the lowest frequency and the

We assume that the energies of ν_{48} vibronic states are given by the anharmonic oscillator expression

TABLE III. The measured S_0 state vibrational frequencies from the emission spectra of isolated *trans,trans*-octatetraene and a comparison with either previously observed solution phase measurements, where available, or theoretically calculated values. All measurements are in units of cm^{-1} .

Assignment	Frequency	Reference 27
ν_{17}	220	219 ^a
ν_{46}	577	565
ν_{45}	384	390
ν_{48}	86.5	96

^aCalculated frequency.

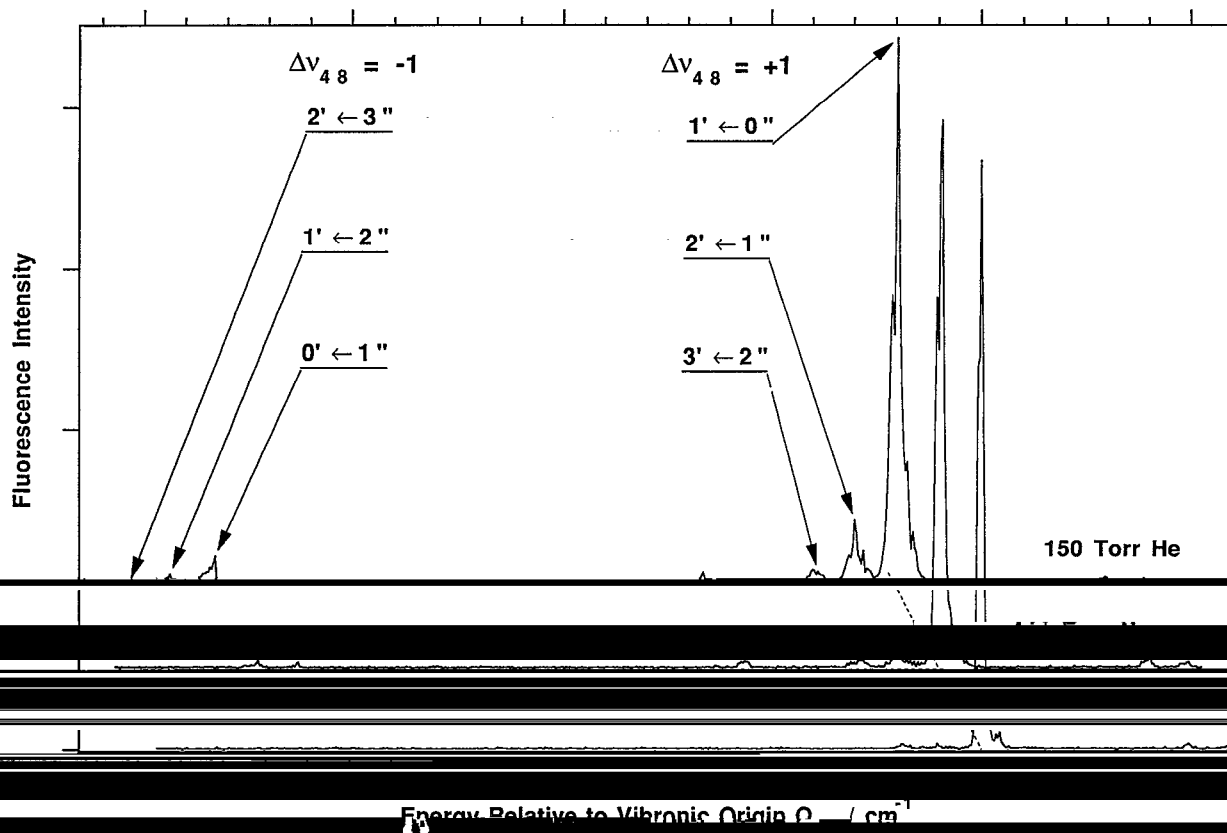


FIG. 5. Fluorescence excitation spectra of the origin region of the 2^1A_g state of octatetraene at He excitation pressures of 150, 300, and 480 Torr. The spectra show the vibrational structure of the 2^1A_g state. The two sequences of bands correspond to $\Delta v = -1$ and $\Delta v = +1$ transitions in the ν_{48} promoting mode.

$$G_v = T_0 + \omega_e(v + \frac{1}{2}) - \omega_e x_e(v + \frac{1}{2})^2, \quad (1)$$

where T_0 contains the contributions to zero-point energy of all modes except for the ν_{48} . The frequency of O_{48} is given by

$$E_{0'-0''} = T_0 + \frac{1}{2}\omega_e' - (\frac{1}{2})^2 \omega_e x_e' - \frac{3}{2}\omega_e'' + (\frac{3}{2})^2 \omega_e x_e''. \quad (3)$$

Using the appropriate relations for the frequencies of other bands, we can derive the following expressions.

$$\Delta_{2''-0''} = E_{1'-0''} - E_{1'-2''} = 2\omega_e'' - 12\omega_e x_e'' = 173.7 \text{ cm}^{-1}, \quad (4)$$

$$\Delta_{2'-0'} = E_{2'-1''} - E_{0'-1''} = 2\omega_e' - 12\omega_e x_e' = 152.8 \text{ cm}^{-1}, \quad (5)$$

$$\Delta_{3'-1'} = E_{2'-2''} - E_{1'-2''} = 2\omega_e' - 20\omega_e x_e' = 171.4 \text{ cm}^{-1}, \quad (6)$$

$$\Delta_{3'-1'} = E_{3'-2''} - E_{1'-2''} = 2\omega_e' - 20\omega_e x_e' = 153.5 \text{ cm}^{-1}. \quad (7)$$

Equations (4)–(7) allow the determination of the harmonic frequencies and anharmonicities for ν_{48} in the ground and excited states, and these can be used to calcu-

late frequency of the $2^1A_g \leftarrow 1^1A_g$ electronic origin (Table IV). The ν_{48}' frequency is exactly the same as the energy difference between the one- and two-photon origins. That the excited state frequency is significantly lower than the ground state frequency and both of the anharmonicities are

negative is consistent with the relative intensity of $\Delta v = -1$ transitions is

TABLE IV. The molecular parameters derived in the analysis of the hot-band structure and their comparison with mixed crystal results. All parameters are in units of cm^{-1} .

Parameter	Molecular beam	Condensed phase
0-0	28 948.7 ^a	28 561 ^b
O_{48}	29 024.9	28 654 ^b
ω_e'	75.9	...
ω_e''	86.3	...
$\omega_e x_e'$	0.089	...
$\omega_e x_e''$	0.090	...
ν_{48}'	76.2	93 ^b
ν_{48}''	86.7	96 ^c

^aThe analysis of hot-band structure and the two-photon spectroscopy give the same energy for the electronic origin of the $S_1 \leftarrow S_0$ spectrum.

^bReference 24.

^cReference 37.

about twice as large as that in $\Delta v = -1$ transitions. This propensity is also seen in the emission spectra.

The assignment of the vibrational hot-band structure to sequence bands in the ν_{48} mode can be verified by other features in the fluorescence excitation and emission spectra. Although $\Delta v > |1|$ transitions are expected to be very weak for antisymmetric vibrations, it is possible to detect a weak band 155.1 cm^{-1} above O_{48} , which may be due to the $3' \leftarrow 0''$ transition in the ν_{48} mode. The difference between $3' \leftarrow 0''$ and O_{48} gives an independent measure of $\Delta_{3,-1}$, from Eq. (7). Further confirmation is provided by emission spectra where $\Delta_{2,-0}$ of 173 cm^{-1} appears in spectra from modes containing one quantum of ν'_{48} (see below).

The hot-band structure and low frequency lines in the fluorescence excitation and emission spectra are only consistent with *trans,trans*-octatetraene. If the spectra were due to the *cis,trans* isomer, then the lowest frequency $0' \leftarrow 1''$ transitions would be shifted from the allowed electronic origin ($0' \leftarrow 0''$) by an amount given by the frequencies of the lowest frequency modes in the condensed phase emission spectra of the *cis,trans* isomer. These are at 29, 51, 120, and

these ground state frequencies. Likewise, the emission spectrum of *trans,trans*-octatetraene in mixed crystals involves

total symmetric modes which build on $b_u 1 \leftarrow 0$ origins. The prominent a_g modes of *trans,trans*-octatetraene in *n*-octane at 4.2 K are at 219 (ν'_{17}), 340 (ν'_{16}), 530 (ν'_{15}), 1221 (ν'_{12}), 1271 (ν'_{11}), and 1754 cm^{-1} (ν'_6) (see Table II).²⁴

must be assigned as sequence bands, since neither isomer is expected to have three vibrations with such closely spaced frequencies. These bands cannot be assigned to the *cis,trans* isomer because (i) there is no known ground state fundamental at 162 cm^{-1} ; (ii) population of several quanta in the 162 cm^{-1} mode would imply a high vibrational temperature and other hot bands that should be observed; (iii)

assignment of the sequence bands to vibrational excitation in the ν_{48} mode of *trans,trans*-octatetraene requires a much lower vibrational temperature and is also consistent with frequencies measured in emission spectra (see below) and the fluorescence excitation spectrum of the cold molecule. The intensity distribution of the hot bands may not be of a statistical ensemble with a well-defined vibrational temper-

2. b_u promoting modes

Other b_u modes also appear as $1 \leftarrow 0$ origins. Vibronic origins due to b_u modes [ν'_{48} (93 cm^{-1}), ν'_{47} (463 cm^{-1}), ν'_{46} (530 cm^{-1}), and ν'_{44} (1054 cm^{-1})] show the following characteristics: (i) they are relatively strong; (ii) they cannot be assigned as overtones or combination bands of lower frequency vibrations; (iii) they do not correspond to any

mentals in two-photon spectra; and (iv) they are origins for progressions in a_g modes with a common intensity pattern, which is also seen for the two-photon spectrum.

In the jet, the corresponding b_u modes have frequencies of 76.2 (ν'_{48}), 439.9 (ν'_{47}), 522.9 (ν'_{46}), and 1044.0 (ν'_{44}) cm^{-1} . Comparison of frequencies for isolated molecules and those in mixed crystals in Table II shows a systematic decrease in the gas phase. In the CC stretching region, ν'_{38} and ν'_{39} also have relatively strong intensities. This is consistent with calculations of S_2 - S_1 coupling matrix elements, which are relatively large for these b_u modes.⁴⁰ However, these are not major features in mixed crystal spectra.

3. Franck-Condon active a_g modes

tra of *trans,trans*-octatetraene in mixed crystals involve totally symmetric modes which build on $b_u 1 \leftarrow 0$ origins. The prominent a_g modes of *trans,trans*-octatetraene in *n*-octane at 4.2 K are at 219 (ν'_{17}), 340 (ν'_{16}), 530 (ν'_{15}), 1221 (ν'_{12}), 1271 (ν'_{11}), and 1754 cm^{-1} (ν'_6) (see Table II).²⁴

the spectrum to *cis,trans*-octatetraene, it would be necessary to invoke large solvent shifts as was done in the 2C-RE2PI study.³⁵ If the spectrum is assigned to the *trans,trans* isomer, only ν'_6 has a significant solvent shift ($+28$ and $+44 \text{ cm}^{-1}$ compared to *n*-hexane and *n*-octane, respectively).²⁴ Since this mode plays an important part in coupling of 1A_g electronic states, its frequency may be very

The vibrational development seen in Figs. 5 and 7 is dominated by combinations and overtones of the most intense a_g modes (ν'_6 , ν'_{12} , and ν'_{16}), which are built on prominent b_u Herzberg-Teller promoting modes (O_{48} , O_{47} ; and O_{46} , O_{39} , and O_{38}). The Franck-Condon activity of these totally symmetric modes is attributed to bond order inversion between the S_0 and S_1 states,^{1-3,26,27} which results in relatively large displacements for these three modes.^{26,40} A

and in combination with other a_g modes up to the second overtone. The contributions of ν'_{12} and ν'_6 to the Franck-Condon development are not so obvious in the fluorescence

However, these two modes dominate the emission spectra (see below). The vibronic intensity in the $S_1 \leftarrow S_0$ spectrum probably occurs for $\Delta v > 0$ in ν'_6 as for methyl substituted tetraenes.¹⁹ The intensity of the ν'_6 fundamental band in the fluorescence excitation spectrum most likely is reduced by faster nonradiative decay at higher excess energies. Other a_g modes such as ν'_{17} at 209.7 cm^{-1} and ν'_{15} at 530.0 cm^{-1} are associated with

involving CC stretches. In contrast to the S_1 state, the ν'_{17} mode is significantly more intense than ν'_{16} in the

4. b_g and a_u modes

The assignments in Table I account for most of the low frequency a_g and b_u vibrational modes. Other low frequency bands which cannot be assigned vibrationally to $trans,trans$ -octatetraene, cannot be assigned to a_g or b_u modes or their combination bands. Emission spectra from these levels terminate in a completely different set of ground state levels, and the lifetimes are significantly dif-

ferent from those of the S_1 state. Their consistent presence in the spectra favors the

assignment of these bands to a_g and b_u modes. First, the appearance of more a_g and b_u bands than can appear as fundamentals in the C_{2h} molecular symmetry

group is an indication that $trans,trans$ -octatetraene is not a planar molecule. The b_g and b_u symmetry species in C_{2h} correspond to the a_g and a_u of C_i . This will

allow for observable transition moments. Second, it is also possible for nontotally symmetric modes to appear as a_g overtones and combination bands if these states borrow intensity by Fermi resonance (unlikely for so many different bands), or if the potential energy surfaces for S_0 and S_1 states have greatly different curvatures. Calculated vibrational fre-

quencies are generally lower than the ground state frequencies and there is significant Duschinsky rotation for the a_u and b_g modes.^{26,43} Extra b_u bands could be due to combination bands of a_g and b_g .

coupling between 2^1A_g and 1^1B_u states. Through these mechanisms, low frequency a_u and b_g modes might have observable intensity,

and their presence in the one- and two-photon spectra indicates a more facile distortion from the

the potential surface for cis- \rightarrow -trans isomerization.

5. Impurity bands

The spectra and detailed assignments given in previous sections establish that the $2^1A_g \rightarrow 1^1A_g$ transition of $trans,trans$ -octatetraene accounts for most of the bands in the fluorescence excitation spectrum. Significant differences between relative intensities in the fluorescence and 2C-RE2PI spectra are found *only* for bands at 33, 49, 236, and 896 cm^{-1} above the origin. The strongest of these lines at 49 cm^{-1} (see the expanded region in Fig. 3) has $\leq 0.3\%$ of the intensity of the corresponding band in the 2C-RE2PI spectrum. Quantitative comparisons of intensities measured by the two techniques are difficult to make because both the ionization cross sections and fluorescence quantum yields are not known. However, different tech-

niques are used. The 49 cm^{-1} fundamental does not appear in combination with other bands, as assigned in the 2C-RE2PI spectrum. In all cases, these bands can be reassigned in a more consistent

C. Analysis of $2^1A_g \rightarrow 1^1A_g$ emission spectra of $trans,trans$ -octatetraene

The emission spectra of the S_1 state of $trans,trans$ -octatetraene are shown in Fig. 6. These spectra show progressions in ν'_{16} , ν'_{12} , and ν'_6 as in the fluorescence excitation spectra. The intensity maxima are shifted 3200–4000 cm^{-1} from the energy of excitation with the most intense transitions being due to combination bands with two quanta of the C–C stretch

of the $2^1A_g \rightarrow 1^1A_g$ spectra of linear polyenes and manifest substantial bond order inversion between the S_1 and S_0 states.^{26,43} Most of the bands seen in the emission spectra involve the three dominant a_g modes and even quanta of one or more of the antisymmetric b_u promoting modes. Transitions can be seen only for the vibrations which differ

by an odd number of quanta. This observation provides further confirmation for the assignment to the $trans,trans$ isomer.

Figures 7 and 8 show details of several spectra that are shown in Table I. Emission spectra from S_1 vibrational levels are dominated by a few common modes which are

observed as a prominent feature in the emission. The intensities of $\Delta v = +1$ transitions in ν_{48} are significantly higher than $\Delta v = 0$ transitions. This is best seen in the emission spec-

trum which is attributed to strong vibronic coupling between the S_1 and

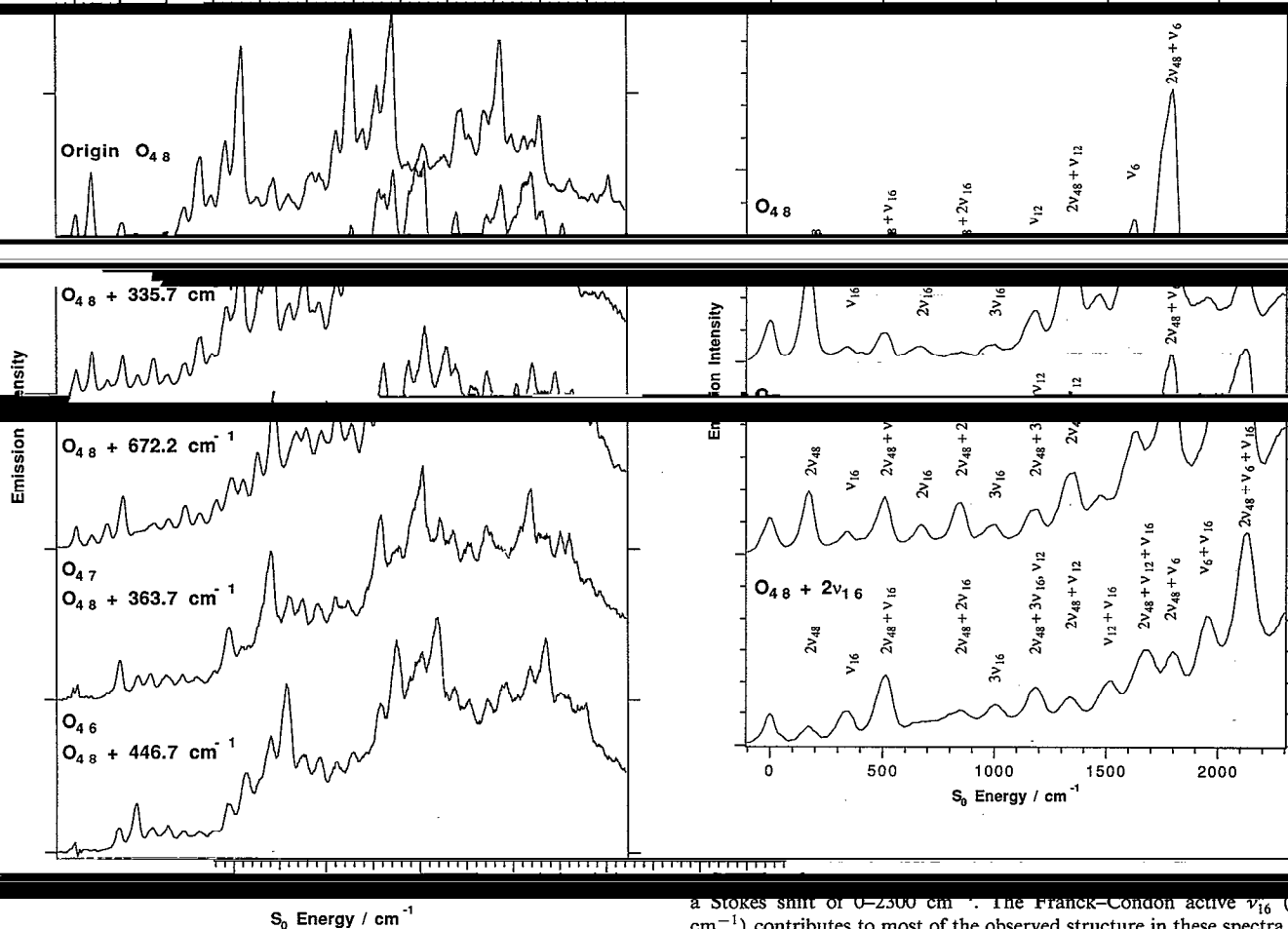


FIG. 6. Representative emission spectra from selected levels in the S_1 state of *trans,trans*-1,3,5,7-octatetraene. The top three spectra originate from $O_{4,8}$ and the first two members of progression additions in the Franck-Condon active modes $O_{4,7}$ and $O_{4,6}$. The emission spectra from the most intense lines can be assigned to progressions in Franck-Condon active ν_{16}'' , ν_{12}'' , and ν_6'' and

S_2 states.^{35,39} This is also supported by analysis of the Raman activity in the corresponding mode of butadiene in resonance with the S_1 state.⁴⁵ Excitation of combination

all other b_g modes. These intensity patterns of low fre-

origins (Fig. 8) also show interesting patterns of vibronic coupling. For emission from $O_{4,8}$, the strongest low frequency line is the $\Delta v = +1$ transition to $2\nu_{48}''$ and the rest of the vibrational structure is dominated by a combination

a Stokes shift of 0–2300 cm^{-1} . The Franck-Condon active ν_{16} (340 cm^{-1}) contributes to most of the observed structure in these spectra. All of the lines involve $\Delta v = \pm 1$ transitions in the ν_{16} promoting mode.

modes. This results in assignment of the vibrational structure in Fig. 9 to binary combinations in b_g modes and their

emissions from $O_{4,7}$ and $O_{4,6}$ ($\Delta v = -1$ in $\nu_{4,7}$ and $\nu_{4,6}$) and

are allowed by symmetry, but have very small transition moments compared to $\Delta v = \pm 1$ in ν_{16} . The frequencies of fundamentals that can be unambiguously identified in the emission spectra are given in Table III. The emission spectra are useful for assigning bands with $< 1000 \text{ cm}^{-1}$ vibra-

spectral congestion in emission spectra.

(Figs. 3 and 4 and Table I) are considerably different from those reported in the 2C-RE2PI experiments.³⁵ In comparison with the fluorescence measurements, lifetimes measured by 2C-RE2PI are much longer (i) 226 fs for

decay rates increase monotonically. Due to rapid mixing of vibrational modes by IVR, the decay rates most likely are determined by vibronic energy rather than the nature of the excited modes. Similar energy dependent increases in decay rates were observed for nonatetraene and decatetraene and attributed to increases in radiative rates due to energy dependent intensity borrowing from the S_2 origin.^{19,21}

At ~ 2100 cm⁻¹ above U_{48} , there is a sharp increase in the rate of fluorescence decay. A similar, but less abrupt threshold was observed for the methyl substituted

substituted derivatives due to a smaller density of vibrational states. The intensity of the fluorescence excitation spectrum drops sharply at this point even though in mixed crystals the absorption strength increases up to the $S_2 \leftarrow S_0$ origin.²⁴

The activated nonradiative decay process above the 2100 cm⁻¹ barrier may be related to the behavior at lower energies. Below 1000 cm⁻¹, there appears to be little correlation between the intensity of bands and their lifetimes. Therefore, it is unlikely that the differences are merely due to the dependence of radiative decay rates on vibronic states. The putative a_u and b_g torsions with anomalous lifetimes may couple to nonradiative channels more

these modes to the S_0 state,¹⁹ or due to coupling with which is believed to occur during *cis-trans* isomerization. The decrease in lifetimes may in part be due to tunnelling through the barrier for isomerization.

The nonradiative decay of *trans,trans*-octatetraene has times has two regimes, both of which depend on the environment (i) in cyclohexane, the lifetimes drop gradually from 126 to 90 ns between 10 and 179 K; and (ii) at higher temperatures, there is a precipitous drop to 2.5 ns at ~ 320 K.^{30,31} The low temperature process has been ascribed to adiabatic isomerization on the S_1 state surface over a barrier of ~ 880 cm⁻¹ to form electronically excited *cis,trans*-octatetraene.^{31,47} A barrier of 1400 cm⁻¹ was determined for the high temperature nonradiative decay pathway, but a mechanism has not been proposed.^{30,31}

the condensed phase may be traced to the same processes that lead to nonradiative decay in isolated octatetraene. The initial drop in the lifetimes at low temperatures in condensed phase may be due to thermal population of the states which are more strongly coupled to nonradiative channels. At higher temperatures, the molecules have sufficient energy to overcome the 1400 cm⁻¹ barrier for the

most and for adiabatic isomerization to *cis,trans*-octatetraene with an 880 cm⁻¹ activation energy on the S_1 surface.

The precipitous drop in the lifetimes at higher energies clearly is due to an activated internal conversion process. A similar phenomenon has been observed for *trans*-stilbene in solution⁴⁸ and under isolated conditions.⁴⁹ The origin of the barrier for isomerization of *trans*-stilbene is believed to be a crossing between the surfaces of the S_1 and a higher

we tentatively propose that the nonradiative decay of isolated *trans,trans*-octatetraene above 2100 cm⁻¹ excess energy also is due to *trans-cis* isomerization.

E. The relative oscillator strengths of $S_1 \leftarrow S_0$ transitions of *cis*- and *trans*-polyenes

The fluorescence excitation spectrum of the $2^1A_g \leftarrow 1^1A_g$ transition of *trans,trans*-octatetraene (Figs. 3 and 4) is almost identical to the 2C-RE2PI spectrum assigned to the $2^1A' \leftarrow 1^1A'$ transition of *cis,trans*-octatetraene.³⁵ The assignment of the 2C-RE2PI spectrum to the *cis,trans* isomer was based, in large part, on the inability of REMPI techniques to detect $S_1 \leftarrow S_0$ spectra of *trans*-isomers of substituted and

orescence and ionization techniques. In this section, we contrast the fluorescence excitation and 2C-RE2PI spectra and discuss the relative oscillator strengths of *cis*- and

The supposition that the $2^1A_g \leftarrow 1^1A_g$ transitions of isolated, *all-trans*-polyenes are too weak to observe³⁵ can be traced to the inability of the REMPI technique to detect the $2^1A_g \leftarrow 1^1A_g$ spectra of *trans*-trienes. There are two possible explanations for the lack of REMPI signals from *trans*-trienes: (i) the transition moments are considerably weaker for the centrosymmetric *all-trans* isomers; and/or (ii) *trans*-trienes undergo rapid internal conversion to the S_0 state. We recently reported the $S_1 \leftarrow S_0$ fluorescence excitation spectra of *cis*-hexatriene and a *cis* isomer of octatriene from samples that contained mostly *trans* isomers.²⁸

hexatriene has at least two separate mechanisms for nonradiative decay—one with no activation energy and another with an activation energy of < 150 cm⁻¹.²⁸ The expected origin of the one-photon $2^1A_g \leftarrow 1^1A_g$ spectrum of *trans*-hexatriene is the $\pi \rightarrow \pi^*$ transition in the lowest frequency b_u mode, with a calculated frequency of 174 cm⁻¹.²⁷ If the activation energy for nonradiative decay

hexatriene would be above this energy. Assuming that *cis* and *trans* hexatriene decay with similar nonradiative decay

hexatriene fluorescence in our experiment.²⁸ We conclude that the $2^1A_g \leftarrow 1^1A_g$ transitions of *all-trans*-trienes have not been observed due to a combination of small transition moments and fast nonradiative decays. Finally, it is impor-

most fluorescent of linear polyenes) based on observations on trienes, considered nonfluorescent until recently.²⁸

Comparison of the relative intensities of the origins of $S_1 \leftarrow S_0$ and $S_2 \leftarrow S_0$ fluorescence excitation spectra in mixed crystals for *cis,trans*- (1:20) and *trans,trans*- (1:10⁵) suggests that the $S_1 \leftarrow S_0$ spectrum is ~ 5000 stronger for the noncentrosymmetric isomer.^{24,29,50} This observation implies that an unattainable level of purity of the *trans,trans* isomer would be necessary to observe the spectrum. Such a comparison of intensities relies on (i) the assumption that the $S_2 \leftarrow S_0$ transition strengths and fluorescence quantum yields are the same for both isomers; (ii) that solutions are optically dilute; and (iii) on correct normalization of fluorescence excitation scans with several laser dyes. Furthermore, the above line of reasoning implies

the $2^1A_g \leftarrow 1^1A_g$ spectrum of any *all-trans* polyene in a

number of experiments that have reported fluorescence excitation and emission spectra from *all-trans* linear polyenes in solutions, low temperature glasses, and mixed crystals.

mers.^{1,23,24,31}

phases also support the conclusion that $S_1 \leftrightarrow S_0$ transitions in *trans*- and *cis*-tetraenes have comparable oscillator strengths. Lifetimes in 10 K alkane solutions are *trans,trans*- 226 ns (*n*-octane) and 123 ns (*n*-hexane); *cis,cis*- 156 ns (*n*-octane), *cis,trans*- 76 ns (*n*-hexane) and *s-cis*- 29 ns (*n*-octane).^{30,51,52} These lifetimes can be compared with the 220 ns radiative lifetime of *trans,trans*-octatetraene determined in room temperature hexane.³²

n-hexane³⁰ is instructive since the $S_1 \leftrightarrow S_0$ spectrum changes from being electronically forbidden to being partially allowed (inversion symmetry is preserved in

yield is not greatly influenced by the solvent). Comparison

symmetry forbidden in *n*-octane), *cis,trans* (symmetry-allowed), and *s-cis* (symmetry-allowed) isomers also indicates relatively small differences in $S_1 \leftrightarrow S_0$ oscillator strengths. For *trans,trans*- and *s-cis*-octatetraene, both the relative fluorescence yields ($\sim 0.36/1$) (Ref. 52) and life-

times are known. These data imply radiative decay rates $k_r \sim 1.0 \times 10^9 \text{ s}^{-1}$ and $k_r \sim 0.36 \times 10^9 \text{ s}^{-1}$.

lifetimes of *trans,trans*- and *cis,trans*-octatetraene suggest an even smaller ratio for the oscillator strengths of their $S_1 \leftrightarrow S_0$ transitions, though the lack of relative fluorescence yields prevents a more quantitative comparison. The measured 220 ns radiative lifetime of *trans,trans*-octatetraene in Table 1 is useful for comparison of transition strengths under isolated conditions. If the two isomers have equal fluorescence quantum yields, the transition strength for the *cis,trans* isomer is at most twice that of the *trans,trans* isomer. The small differences in fluorescence lifetimes for systems with and without inversion symmetry indicate that the S_1 lifetimes are determined primarily by vibronic coupling with the S_2 state and that this coupling is not very sensitive to the excited state geometries.

V. CONCLUSIONS

Fluorescence excitation and emission spectra of the $S_1 \leftrightarrow S_0$ transitions of *trans,trans*-1,3,5,7-octatetraene have

been reported previously and been obtained in a 10 K matrix.

$2^1A_g \leftarrow 1^1A_g$ transition of *trans,trans*-octatetraene is based on (i) comparison of the one- and two-photon fluorescence excitation spectra; (ii) vibronic analysis of the one-photon

photon fluorescence excitation spectra in the condensed phase; (iii) analysis of $S_1 \rightarrow S_0$ emission spectra from a

rescence lifetimes; and (v) the $S_2 \leftarrow S_0$ fluorescence excitation spectrum. The analysis of the spectra provides important structural information on isolated *trans,trans*-octatetraene such as accurate frequencies for a number of a_g and b_u vibrations and the electronic origin of the S_1 state.

The dominance of $2^1A_g \leftarrow 1^1A_g$ transitions in the lowest frequency b_u in-plane bending vibration (ν_{11}) in the gas

strong Herzberg-Teller coupling between the S_2 and S_1 states. The fluorescence lifetimes of individual S_1 vibronic states depend on the vibronic level excited in the low en-

The discovery of $2^1A_g \rightarrow 1^1A_g$ emissions in gaseous trienes,²⁸ tetraenes, and pentaenes¹⁸ now has led to the detection of the $2^1A_g \leftarrow 1^1A_g$ transitions of several polyenes in supersonic jets using fluorescence excitation techniques.^{19,20,28} These experiments have provided the first de-

